

Detecting dark matter oscillations with gravitational waveforms

Philippe Brax and Patrick Valageas

Université Paris-Saclay, CNRS, CEA, Institut de physique théorique, 91191, Gif-sur-Yvette, France

Clare Burrage

School of Physics and Astronomy, University of Nottingham, Nottingham, NG7 2RD, United Kingdom

Jose A. R. Cembranos,

*Departamento de Física Teórica and IPARCOS, Facultad de Ciencias Físicas,
Universidad Complutense de Madrid, Ciudad Universitaria, 28040 Madrid, Spain*

We consider the phase shift in the gravitational wave signal induced by fast oscillations of scalar dark matter surrounding binary systems, which could be probed by the future experiments LISA and DECIGO. This effect depends on the local matter density and the mass of the dark matter particle. We compare it to the phase shift due to a standard dynamical friction term, which should generically be present. We find that the effect associated with the oscillations only dominates over the dynamical friction for dark matter masses below 10^{-21} eV, with masses below 10^{-23} eV implying cloud sizes that are too large to be realistic. Moreover, for masses of the order of 10^{-21} eV, LISA and DECIGO would only detect this effect for dark matter densities greater than that in the solar system by a factor 10^5 or 10^4 respectively. We conclude that this signal can be ignored for most dark matter scenarios unless very dense clouds of very light dark matter are created early in the Universe at a redshift $z \sim 10^4$.

I. INTRODUCTION

The exploration of dark matter (DM) halos as scalar field solitons of extended sizes has emerged as a promising avenue to test the fundamental nature of DM. Recent studies have investigated this possibility as an alternative framework addressing some of the small-scale observational challenges of the conventional Cold DM scenario [1, 2]. Indeed Scalar DM models, distinguished by a background oscillating field whose pulsation is determined by the mass of the scalar particle, introduce a novel perspective on the dynamics of DM [3]. Although these oscillations manifest themselves at rapid rates on cosmological and astrophysical scales, a common analytical strategy involves integrating them out, focusing on the slow temporal and spatial variations in the amplitude of the scalar field for a more manageable analysis [4–6].

The framework used in this work includes the popular fuzzy DM (FDM) models as an alternative to the traditional cold DM paradigm [7]. FDM, characterized by ultralight bosonic DM constituents within the mass range $10^{-22} - 10^{-20}$ eV, has garnered attention due to its unique description based on a single coherent wavefunction [8, 9]. Numerical simulations have demonstrated that FDM, on large scales, reproduces the cosmic web structure of CDM while addressing challenges faced by CDM on galactic scales [8–10]. Favourable aspects of FDM, such as resolving the cusp-core problem [11], have led to an increased interest in its potential to remedy purported issues with the CDM model [12–14]. This has sparked extensive research into the dynamics of FDM solitons, also known as cores, within halos [15–18]. The cores in FDM halos exhibit intriguing dynamical behaviors, including random walks within the gravitational potential and stochastic features [8, 9, 19–24], as well as

homogeneous radial expansions and contractions of the soliton core, sending out density waves into the surrounding halo [21].

Historically, most investigations of FDM have considered non-interacting bosons, described by a Schrödinger equation coupled to the Poisson equation in the Schrödinger-Poisson system of coupled equations (SPE) [25–36]. However, recent efforts have explored the dynamical effects introduced by interactions, which add nonlinear contributions to the Schrödinger equation [25–36]. Such interactions lead to a more complex and dynamically rich scenario. After integrating out the fast oscillations of the scalar field, the dynamics of DM can be understood as the one of a fluid, where equilibria arise from the balance between gravity, self-interactions, and the ‘quantum-pressure’ resulting from the spatial gradients of the scalar. These solitons could play a significant role in shaping the large-scale structure of the universe. The Fuzzy DM solitons are associated to the balance between quantum-pressure and gravity [37]. Other solitons where repulsive self-interactions equilibrate with gravity provide alternative examples [6].

In this article, we consider scalar field solitons and their influence on astrophysical phenomena, in particular the propagation of gravitational waves (GW). Small solitons, whose sizes could be significantly smaller than galactic halos and could be formed during different cosmic eras, e.g the matter or radiation eras [38], could modify the phase of GW produced by binary systems. These solitons, exhibiting densities much larger than the average DM density in galactic halos, may constitute a significant portion of the total DM in the universe. For instance, if formed around the time of matter-radiation equality, they could reach densities as high as one million times the local DM density in the solar system. We specifically

focus on binary systems that could potentially belong to these dense clumps and the effects on the GWs they produce that could be probed by future experiments like LISA [39] and DECIGO [40]. We note that the capture of binary systems by these dense clumps remains a subject for future study.

Environmental effects, associated with baryons or dark matter, generically affect the gravitational waves signal emitted by binary systems via their impact on the orbital features. Typically, they are the consequences of three possible effects, the conservative gravitational pull of the enclosed dark matter mass within the binary orbit, the dynamical friction (i.e., the drag force on the binary components due to the gravitational exchange of momentum with the environment), or the accretion of matter. Recent studies of these effects can be found for instance in [41–46]. In this paper, following [47], we focus on a different effect that is specific to scalar field scenarios (as opposed to classical particles or fluids) and associated with the fast oscillations of the scalar field $\phi(\vec{x}, t)$, which can be written as

$$\phi(\vec{x}, t) = A(\vec{x}, t) \cos[m_\phi t + \alpha(\vec{x}, t)]. \quad (1)$$

where m_ϕ is the dark matter particle mass. The amplitude A and the phase α vary on astrophysical or cosmological timescales. Similarly the dark matter density and the gravitational field, when averaged over the fast oscillations of the scalar field at frequency m_ϕ , vary also on such large time scales. As recalled above, the dynamics of the dark matter density field, such as the formation of solitons, are usually studied using the equations of motion obtained after this averaging procedure, written in terms of the amplitude A and the phase α or the complex field $\psi = Ae^{i\alpha}$. However, as pointed out by [47], the underlying fast oscillations (1) lead to a subleading oscillating component of the gravitational potential Ψ_N , as in Eq.(3) below. This in turns gives rise to a specific time-dependent shift of the gravitational waveform, which is not due to a change of the orbital dynamics but to the propagation of the gravitational wave in the surrounding oscillating gravitational potential.

In this paper, we compute this specific phase shift and we compare its magnitude with a generic dynamical friction [45, 48, 49]. Interestingly, we find that the oscillating DM effects can only be probed for a specific range of scalar masses, dependent on the GW frequency and the total mass of the binary system. Practically, our results suggest that only scalar masses lower than 10^{-21} eV could be tested when the local matter density exceeds one million times the estimated density for DM in the Milky Way. The formation of very dense clumps around the matter-radiation equality epoch would then lead to potentially observable effects. Our analysis applies to scenarios of the form (1), which include both FDM models and models with non-negligible self-interactions.

In Section II, we compute the shift in the frequency and phase of the gravitational waves due to the oscillating dark matter background, and compare this to the size of

similar effects arising from dynamical friction. In Section III, we use a Fisher matrix analysis to determine which local dark matter overdensities can be probed with near future experiments, focusing in particular on LISA and DECIGO. We conclude in Section IV.

II. IMPACT OF THE TIME-DEPENDENT DARK MATTER POTENTIAL ON GW

A. Frequency shift

In the near future the LISA experiment will detect and analyse the GWs due to white dwarf binaries in the Milky Way. It is expected that over 10 years of observation, some 10^4 White Dwarf Binaries (WDB) will be observed at frequencies $f_0 \gtrsim 5$ mHz [50, 51]. These systems will allow us to test the nature of their DM environment [47]. In a fashion similar to the Sachs-Wolfe effect for the Cosmic Microwave Background (CMB), the fluctuations of the gravitational potential along the line of sight lead to a drift of the frequency, f , of the emitted GWs,

$$\frac{\Delta f}{f} = \Psi_N(\vec{x}, t) - \Psi_N(\vec{x}_e, t_e), \quad (2)$$

where $\{\vec{x}_e, t_e\}$ and $\{\vec{x}, t\}$ indicate the position and time of the emission and reception of the GW. This description is valid as long as the GWs can be described as rays in an optical approximation where their frequency must be larger than the inverse of the typical variation scale of the surrounding medium. The integrated Sachs-Wolfe effect is also neglected. This follows from the fact that the spatial variation of the gravitational potential occurs on scales much larger than the wavelength.

If the galactic halo is composed of clumps of DM whose particle mass is m_ϕ , the local matter density will include a subleading component that oscillates with a frequency $\omega = 2m_\phi$ locally inside each clump, associated with the underlying oscillation (1) of the field. Through the Einstein equations we find the local Newtonian potential to be [47]

$$\Psi_N(\vec{x}, t) = \Psi_0(\vec{x}) + \Psi_{\text{osc}}(\vec{x}) \cos[\omega t + 2\alpha(\vec{x})], \quad (3)$$

with

$$\omega = 2m_\phi. \quad (4)$$

The leading component in Eq. (3), Ψ_0 , which evolves on astrophysical timescales, is given by the usual Poisson equation,

$$\nabla^2 \Psi_0 = 4\pi \mathcal{G} \rho, \quad (5)$$

where ρ is the DM density averaged over the fast oscillations at frequency ω , whereas the subleading oscillating component Ψ_{osc} is given by

$$\Psi_{\text{osc}} = \pi \frac{\mathcal{G} \rho}{m_\phi^2}. \quad (6)$$

The de Broglie wavelength λ_{dB} of the DM particles is $\lambda_{\text{dB}} = 2\pi/(m_\phi v)$, with v the typical virial velocity of the DM cloud. The effective quantum pressure smoothes out inhomogeneities on scales smaller than λ_{dB} , therefore typical wavenumbers k of the DM density field verify $k < 2\pi/\lambda_{\text{dB}}$ (k can be much smaller if there are repulsive self-interactions that contribute to an additional pressure, or more generally as in CDM scenarios when the size of the cloud is related to its formation process rather than to m_ϕ). Then, comparing equations (5) and (6) we have

$$k < \frac{2\pi}{\lambda_{\text{dB}}} : \quad k < m_\phi v, \quad \frac{\Psi_{\text{osc}}}{\Psi_0} \sim \frac{k^2}{m_\phi^2} < v^2 \ll 1, \quad (7)$$

for nonrelativistic DM clouds.

As pointed out in Ref. [47] in the context of Pulsar Timing Arrays (PTAs), the oscillating component Ψ_{osc} will lead, through Eq. (2), to an oscillating frequency drift of the GW, which could be detected, whereas the constant term Ψ_0 is degenerate with binary parameters. We shall find below that a detection requires a DM density that is much larger than the solar neighborhood estimate. Therefore, we can assume the gravitational potential at emission to dominate in Eq. (2) and we write the observed frequency of the GW signal as

$$f = \bar{f} + \Delta f = \bar{f}(1 + \Psi), \quad (8)$$

where \bar{f} is the unperturbed frequency, that is, for a binary system in vacuum, and Δf is the frequency shift due to the binary DM environment, with

$$\Psi = \Psi_0 + \Psi_{\text{osc}} \cos(\omega t - \theta), \quad (9)$$

where $\theta = -2\alpha(\vec{x}_e) - \pi$ and we redefined Ψ_0 with a change of sign. The optical approximation (2) is valid for

$$f \gtrsim \omega, \quad \text{whence } m_\phi < \left(\frac{f_{\text{min}}}{1 \text{ Hz}}\right) 3 \times 10^{-16} \text{ eV}, \quad (10)$$

where f_{min} is the minimum frequency of the GW interferometer. Compared with the contributions from Eq. (2), the integrated Sachs-Wolfe effect is suppressed by a factor $k/\omega < v \ll 1$ and can be neglected for nonrelativistic clouds.

Throughout this paper, we work at linear order in the DM density and gravitational potential. Our analysis is not restricted to the clouds associated with solitons in Fuzzy DM scenarios (i.e., stable equilibria governed by the balance between gravity and quantum pressure). It also applies to more general cases, such as solitons governed by the balance between gravity and the effective pressure due to repulsive self-interactions, or virialized halos supported by their velocity dispersion (as for CDM).

B. Gravitational wave phase shift

The GW signal from the binary systems we consider takes the form $h(t) = A(t) \cos[\Phi(t)]$, where the phase

$\Phi(t)$ and the time t are related to the frequency f and the frequency drift \dot{f} by

$$\Phi = 2\pi \int df \frac{f}{\dot{f}}, \quad t = \int df \frac{1}{\dot{f}}. \quad (11)$$

At leading order, the amplitude grows as $A(t) \propto f^{2/3}$ and the frequency drift due to the emission of GW by the binary system reads

$$\dot{f} = \frac{96\pi^{8/3}}{5c^5} (\mathcal{G}\mathcal{M})^{5/3} f^{11/3}, \quad (12)$$

where \mathcal{M} is the chirp mass of the two compact objects of mass m_1 and m_2 , and

$$M = m_1 + m_2, \quad \nu = m_1 m_2 / M^2, \quad \mathcal{M} = \nu^{3/5} M, \quad (13)$$

where ν is the symmetric mass ratio [49, 52].

Going to Fourier space, $\tilde{h}(f) = \int dt e^{i2\pi f t} h(t)$, one obtains in the stationary phase approximation $\tilde{h}(f) = A(f) e^{i\psi(f)}$ with

$$A(f) \propto f^{-7/6}, \quad \psi(f) = 2\pi f t_\star - \Phi(t_\star) - \pi/4, \quad (14)$$

where the saddle-point t_\star is determined by $f(t_\star) = f$.

At zeroth order in the DM environment, we have $\tilde{f}(\bar{t}_\star) = f$ and

$$t_c - \bar{t}_\star = \int_f^\infty df \frac{1}{\dot{f}} = \frac{5}{256\pi} \left(\frac{\pi\mathcal{G}\mathcal{M}}{c^3}\right)^{-5/3} f^{-8/3}, \quad (15)$$

with the phase given by

$$\Phi_c - \bar{\Phi}_\star = 2\pi \int_f^\infty df \frac{f}{\dot{f}} = \frac{1}{16} \left(\frac{\pi\mathcal{G}\mathcal{M}f}{c^3}\right)^{-5/3}, \quad (16)$$

where t_c and Φ_c are the time and the phase at that coalescence time. This gives the standard result for the phase $\bar{\psi}(f)$ of the Fourier-space waveform:

$$\bar{\psi}(f) = 2\pi f t_c - \Phi_c - \frac{\pi}{4} + \psi_{\text{GW}}(f) \quad (17)$$

with

$$\psi_{\text{GW}}(f) = \frac{3}{128} \left(\frac{\pi\mathcal{G}\mathcal{M}f}{c^3}\right)^{-5/3} \left[1 + \left(\frac{3715}{756} + \frac{55\nu}{9}\right) \times \left(\frac{\pi\mathcal{G}\mathcal{M}f}{c^3}\right)^{2/3} \right]. \quad (18)$$

Here we have included the first post-Newtonian correction (1-PN order). This gives two terms, which behave as $f^{-5/3}$ and f^{-1} , that allow us to constrain both binary masses m_1 and m_2 from the observations [45]. We do not consider higher order post-Newtonian contributions in this paper, which can be used to constrain the spins of the compact objects.

Because of the DM perturbation Eq. (8), the saddle-point time t_* associated with a frequency f is shifted at first order by

$$t_* = \bar{t}_* + \Delta t_*, \quad \text{with} \quad \Delta t_* = -\frac{\bar{f}(\bar{t}_*)}{f'(\bar{t}_*)}\Psi(\bar{t}_*), \quad (19)$$

while the phase $\Phi_* = \bar{\Phi}_* + \Delta\Phi_*$ is shifted by

$$\Delta\Phi_* = 2\pi f\Delta t_* - 2\pi \int_{\bar{t}_*}^{t_c} dt \bar{f}\Psi. \quad (20)$$

This gives a shift of the phase $\Delta\psi(f)$ of the Fourier-space waveform

$$\Delta\psi(f) = 2\pi \int_{\bar{t}_*}^{t_c} dt \bar{f}\Psi. \quad (21)$$

Using Eq. (15), we can write this integral as

$$\Delta\psi = 2\pi \left(\frac{5}{256\pi}\right)^{3/8} \left(\frac{\pi\mathcal{G}\mathcal{M}}{c^3}\right)^{-5/8} \int_{\bar{t}_*}^{t_c} dt (t_c - t)^{-3/8} \Psi(t). \quad (22)$$

The constant term Ψ_0 of the gravitational potential in Eq. (9) gives the contribution

$$\Delta\psi_0(f) = \frac{\Psi_0}{16} \left(\frac{\pi\mathcal{G}\mathcal{M}f}{c^3}\right)^{-5/3}. \quad (23)$$

We can see that this term, which scales as $f^{-5/3}$, is fully degenerate with the leading GW phase in Eq. (18). Moreover, for nonrelativistic DM clouds $\Psi_0 \ll 1$. Therefore, we would need to know the distribution of white dwarf masses (or more generally binary masses) with a very high accuracy to distinguish the effect of the contribution (23). Thus Ψ_0 cannot be discriminated from a small shift of the binary masses m_1 and m_2 and we do not consider it any further.

The time-dependent term of the gravitational potential in Eq. (9) gives the contribution

$$\begin{aligned} \Delta\psi_{\text{osc}}(f) &= \Psi_{\text{osc}} 2\pi \left(\frac{5}{256\pi}\right)^{3/8} \left(\frac{\pi\mathcal{G}\mathcal{M}\omega}{c^3}\right)^{-5/8} \\ &\quad \times \text{Re} \left[e^{i(5\pi/16 + \theta - \omega t_c)} \gamma(5/8, -iy) \right], \end{aligned} \quad (24)$$

where $\gamma(a, z)$ is the incomplete gamma function and

$$y = \omega(t_c - \bar{t}_*) = \frac{m_\phi}{m_*}, \quad m_* = f \frac{128\pi}{5} \left(\frac{\pi\mathcal{G}\mathcal{M}f}{c^3}\right)^{5/3}. \quad (25)$$

For low scalar mass, $m_\phi \ll m_*$, we obtain

$$m_\phi \ll m_* : \quad \Delta\psi_{\text{osc}}(f) = \frac{\Psi_{\text{osc}}}{16} \left(\frac{\pi\mathcal{G}\mathcal{M}f}{c^3}\right)^{-5/3} \cos(\omega t_c - \theta). \quad (26)$$

Because of the bounds in Eq. (7), this phase shift is even smaller than for the constant potential contribution of

Eq. (23) and it is again degenerate with the GW phase in Eq. (18). For high scalar masses, $m_\phi \gg m_*$, we obtain

$$\begin{aligned} m_\phi \gg m_* : \quad \Delta\psi_{\text{osc}}(f) &= \Psi_{\text{osc}} \Gamma(5/8) 2\pi \left(\frac{5}{256\pi}\right)^{3/8} \\ &\quad \times \left(\frac{\pi\mathcal{G}\mathcal{M}\omega}{c^3}\right)^{-5/8} \cos(\omega t_c - \theta - 5\pi/16), \end{aligned} \quad (27)$$

which is degenerate with the constant factor Φ_c in Eq. (17). Therefore, the DM phase shift is degenerate in both low and high scalar mass limits. This means that the contribution of the DM environment binary gravitational wave forms can only potentially be distinguished for scalar masses of the order of m_* , which can span a few orders of magnitude depending on the frequency range of the GW interferometer. Notice that this typical mass m_* is much smaller than the signal's frequency as long as the GWs do not probe the Schwarzschild radius of the system. This must of course be satisfied for our semi-classical description of the propagation of the GWs to hold.

C. Comparison with dynamical friction

If a binary system is embedded within a DM halo, its GWs signal will be affected by other, more usual, effects, in addition to the phase shift in Eq. (24) associated with the specific oscillatory behavior of the Newtonian potential in Eq. (3). These include the impact of the DM halo on the orbital radius of the binary, due to gravitational force from the enclosed DM mass, the matter accretion onto the compact objects, and the dynamical friction. The rate of matter accretion can depend on the details of the DM model but the dynamical friction often takes the form of the usual Chandrasekhar result [48]

$$m_i \dot{\vec{v}}_i = -\frac{4\pi\mathcal{G}^2 m_i^2 \rho}{v_i^3} \Lambda \vec{v}_i, \quad (28)$$

where Λ is the Coulomb logarithm and the index $i = \{1, 2\}$ labels the two components of the binary system. The expression in Eq. (28) derived for collisionless media, such as CDM, also applies to Fuzzy DM or scenarios with non-negligible self-interactions in the supersonic regime, although Λ depends on the model. Therefore, it is interesting to compare the the phase shift we derived in Eq. (24) with the generic effect of the dynamical friction, Eq. (28), which is expected to be also present in most cases. To keep the analysis general and simple, we approximate Λ as a constant, and in our numerical computations we will take $\Lambda = 10$. As described for instance in Ref. [45], the drag force, Eq. (28), leads to a slow decay of the orbital radius a , in addition to the shrinking due to the emission of GWs, which reads

$$\dot{a}_{\text{df}} = -a \left(\frac{a}{\mathcal{G}M}\right)^{3/2} 8\pi\mathcal{G}^2 \rho \Lambda \frac{m_1^3 + m_2^3}{\mu^2}, \quad (29)$$

where $\mu = m_1 m_2 / M$ is the reduced mass. This in turn gives rise to an additional drift of the GWs frequency;

$$\dot{f}_{\text{df}} = 12\mathcal{G}\rho \frac{\Lambda(m_1^3 + m_2^3)}{\nu^{1/5}\mathcal{M}^3}, \quad (30)$$

and to a phase shift;

$$\Delta\psi_{\text{df}} = -\frac{75}{38912} \frac{\pi\mathcal{G}^3\mathcal{M}\rho}{c^6} \left(\frac{\pi\mathcal{G}\mathcal{M}f}{c^3}\right)^{-16/3} \frac{\Lambda(m_1^3 + m_2^3)}{\nu^{1/5}\mathcal{M}^3}. \quad (31)$$

Here, as in [45], we consider the effects due to DM as a linear perturbation to the GW emission and assumed that the contribution of Eq. (30) to the frequency drift is small as compared with the contribution of Eq. (12) due to the emission of GWs.

III. DETECTION THRESHOLD

A. Fisher matrix analysis

We use a Fisher matrix analysis to investigate which DM densities can be probed by GW waveforms, through the impact of the oscillating Newtonian potential in Eq. (9) on the phase of Eq. (24). As usual [53, 54], the Fisher matrix reads

$$\Gamma_{ij} = 4 \text{Re} \int_{f_{\text{min}}}^{f_{\text{max}}} \frac{df}{S_n(f)} \left(\frac{\partial \tilde{h}}{\partial \theta_i}\right)^* \left(\frac{\partial \tilde{h}}{\partial \theta_j}\right), \quad (32)$$

where $S_n(f)$ is the noise spectral density of the GW interferometer and $\{\theta_i\}$ is the set of parameters that we wish to measure. In this paper we consider $\{\theta_i\} = \{t_c, \Phi_c, \ln(m_1), \ln(m_2), \Psi_{\text{osc}}\}$, as we discard the spins of the compact objects. The amplitude \mathcal{A}_0 would be an additional parameter, however, the Fisher matrix is block-diagonal as $\Gamma_{\mathcal{A}_0, \theta_i} = 0$ and the amplitude \mathcal{A}_0 is completely decorrelated from the other parameters $\{\theta_i\}$ [53]. Therefore, we do not consider the amplitude any further. From the Fisher matrix Γ_{ij} we obtain the covariance matrix $\Sigma_{ij} = (\Gamma^{-1})_{ij}$, which gives the standard deviation on the various parameters as $\sigma_i = \langle (\Delta\theta_i)^2 \rangle^{1/2} = \sqrt{\Sigma_{ii}}$. We obtain in this fashion the 1-sigma error bar on the amplitude of the DM oscillating potential Ψ_{osc} , or equivalently on the DM density ρ through Eq. (6). We perform the analysis for a fiducial $\rho = 0$, i.e. assuming the binary is in vacuum. Then, we identify σ_ρ as the detection threshold on the DM density ρ .

The signal-to-noise ratio is given by

$$(\text{SNR})^2 = 4 \int_{f_{\text{min}}}^{f_{\text{max}}} \frac{df}{S_n(f)} |\tilde{h}(f)|^2. \quad (33)$$

Writing the GWform as $\tilde{h}(f) = \mathcal{A}_0 f^{-7/6} e^{i\psi(f)}$ at leading order, we obtain the standard expression

$$\Gamma_{ij} = \frac{(\text{SNR})^2}{\int_{f_{\text{min}}}^{f_{\text{max}}} \frac{df}{S_n(f)} f^{-7/3}} \int_{f_{\text{min}}}^{f_{\text{max}}} \frac{df}{S_n(f)} f^{-7/3} \frac{\partial \psi}{\partial \theta_i} \frac{\partial \psi}{\partial \theta_j}. \quad (34)$$

The derivatives are computed from Eqs.(17), (18) and (24), which we simplify as

$$\Delta\psi_{\text{osc}}(f) \sim \Psi_{\text{osc}} 2\pi \left(\frac{5}{256\pi}\right)^{3/8} \left(\frac{\pi\mathcal{G}\mathcal{M}2m_\phi}{c^3}\right)^{-5/8} \times \left| \gamma \left(\frac{5}{8}, -i\frac{m_\phi}{m_\star(f)}\right) \right|, \quad (35)$$

where we have discarded the random phase factor and directly compute the modulus of the term in the real part. This provides the order of magnitude of the phase shift associated with the DM environment, through the impact of the oscillating gravitational potential. As we take $\Psi_{\text{osc}} = 0$ as the fiducial case, the derivatives in Eq. (34) with respect to $\{t_c, \Phi_c, \ln(m_1), \ln(m_2)\}$ arise from the zeroth-order terms, Eqns. (17) and (18), whereas the derivative with respect to Ψ_{osc} is given by (35).

To compare with the impact of dynamical friction, Eq. (31), we also perform a separate Fisher analysis where we only include the phase shift in Eq. (31) for the impact of DM. Then we consider the parameters $\{\theta_i\} = \{t_c, \Phi_c, \ln(m_1), \ln(m_2), \rho\}$ and we directly obtain the detection threshold σ_ρ on the DM density ρ , which does not depend on the particle mass m_ϕ .

B. LISA

	m_1 (M_\odot)	m_2 (M_\odot)	SNR
MBBH	10^6	5×10^5	3×10^4
IBBH	10^4	5×10^3	708
IMRI	10^4	10	64
EMRI	10^5	10	22
WD	0.4	0.3	7

TABLE I. Masses and SNR (Signal-to-Noise Ratio) of the events that we consider for LISA.

We now consider various binary systems that should be observed by the LISA interferometer: Massive Binary Black Holes (MBBH), Intermediary Binary Black Holes (IBBH), Intermediate Mass Ratio Inspiral (IMRI), Extreme Mass Ratio Inspiral (EMRI), and White Dwarfs binaries (WD). We give in Table I the masses and SNR of typical events that we use for the numerical computations.

We show in the upper panel in Fig. 1 our results for the detection threshold on the oscillating DM gravitational potential Ψ_{osc} , for these events. The vertical blue dotted line is the upper boundary, Eq. (10), for the MBBH case. For other events this upper boundary is located to the right of the DM particle mass range shown in the picture. As explained in Sec. II B, the phase shift of Eq. (24) due to the DM oscillating gravitational potential is degenerate at low and high masses with the standard result. Thus, the amplitude Ψ_{osc} is poorly constrained at low

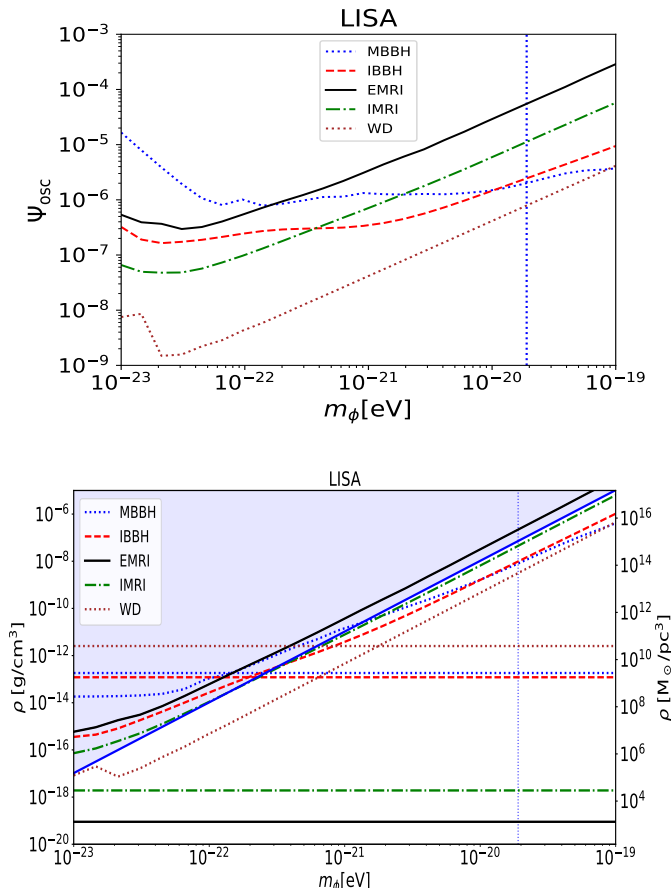


FIG. 1. Detection thresholds on the amplitude Ψ_{osc} of the oscillating DM gravitational potential (upper panel) and on the DM density ρ (lower panel), as a function of the scalar mass m_ϕ . We show the results obtained for various events with the LISA interferometer. In the lower panel, the shaded blue area is the exclusion region associated with the upper bound (37) with $M_{\text{cloud}} = 10^7 M_\odot$.

and high masses and the best constraints are obtained for $m_\phi \sim 10^{-22}$ eV. We do not consider masses below 10^{-23} eV because they cannot constitute a large fraction of the DM (the de Broglie wavelength would be greater than galactic cores). In agreement with Eq. (25), MBBH and IBBH events, which have a greater chirp mass \mathcal{M} , probe somewhat higher scalar masses than EMRI and IMRI events. White Dwarfs have smaller mass than these massive BHs. This increases the phase shift (35) and improves the detection threshold, in agreement with our numerical result shown in Fig. 1.

We show in the lower panel in Fig. 1 our results for the detection threshold on the DM density ρ . From Eq. (6) we have $\sigma_\rho \propto m^2 \sigma_{\Psi_{\text{osc}}}$. This leads to the very fast growth with m_ϕ of the detection threshold σ_ρ . In addition to these curves, the horizontal lines show the detection thresholds associated with the dynamical friction, Eq. (31), which are independent of m_ϕ . We can see that for $m_\phi \gtrsim 10^{-21}$ eV dynamical friction is more im-

portant than the oscillatory gravitational potential. For EMRIs and IMRIs this is actually the case at all masses. As compared with the DM density in the solar neighborhood, $\rho \sim 1 M_\odot/\text{pc}^3$, LISA can only detect DM densities that are higher by a factor of at least 10^5 . Such DM clouds may be formed at high redshifts, $z \sim 10^4$. This would correspond to the matter density at the formation time when such clumps form by a rapid instability, e.g. tachyonic [38]. However, their very large radii make such a scenario somewhat unlikely. Indeed, we can expect their radius to be greater than the Compton wavelength,

$$\lambda_C = \frac{2\pi}{m_\phi} = \left(\frac{m_\phi}{1 \text{ eV}}\right)^{-1} 4 \times 10^{-23} \text{ pc}. \quad (36)$$

For $m_\phi \sim 10^{-22}$ eV, as for Fuzzy DM scenarios, this corresponds to clouds of parsec size or greater. They would be smaller than globular clusters, which can reach sizes of 100 pc, but denser by a factor 10^3 . The comparison between the Compton and de Broglie wavelengths, $\lambda_{\text{dB}} = \lambda_C/v$, suggests that clouds with $R \sim \lambda_C$ would also be relativistic. For a given mass M_{cloud} of the DM cloud, the inequality $R > \lambda_c$ of the cloud radius gives the upper bound

$$\rho = \frac{M_{\text{cloud}}}{R^3} < \frac{M_{\text{cloud}}}{\lambda_c^3} = \frac{M_{\text{cloud}}}{1 M_\odot} \left(\frac{m_\phi}{1 \text{ eV}}\right)^3 10^{45} \text{ g/cm}^3. \quad (37)$$

We show this upper bound with $M_{\text{cloud}} = 10^7 M_\odot$ by the blue shaded area in the lower panel in Fig. 1. Thus, we can see that the high densities required to detect the phase shift $\Delta\psi_{\text{osc}}$ also imply very high cloud masses, $M_{\text{cloud}} \gtrsim 10^5 M_\odot$ for WD binaries.

C. DECIGO

	$m_1 (M_\odot)$	$m_2 (M_\odot)$	SNR
GW150914	35.6	30.6	2815
GW170608	11	7.6	1290
GW170817	1.46	1.27	2124

TABLE II. Masses and SNR of the events that we consider for DECIGO.

We also consider stellar-mass BH and neutron star events that could be detected by the DECIGO interferometer. We choose as typical cases three events detected by LIGO and Virgo [55] given in Table II.

We show in Fig. 2 our results for the detection thresholds on the oscillating DM gravitational potential Ψ_{osc} and the density ρ , for various events with the DECIGO interferometer. For all events the upper boundary, Eq. (10), is located to the right of the DM particle mass range shown in the picture. The thresholds for DECIGO and LISA are of about the same orders of magnitude, although they are somewhat more favorable for DECIGO.

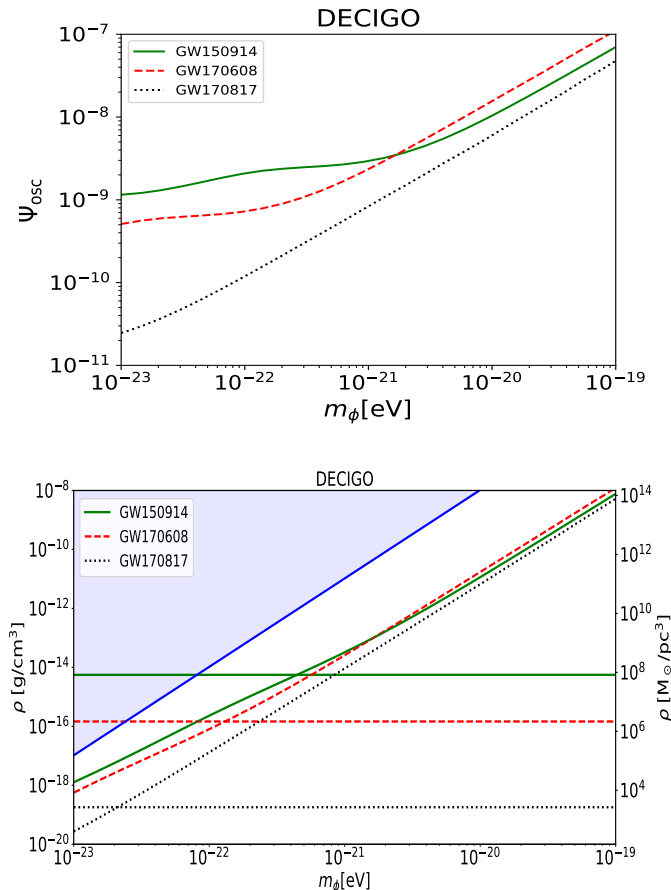


FIG. 2. DM detection thresholds as in Fig. 1 but for the DECIGO interferometer.

In particular, the required DM density are further below the upper bound of Eq. (37).

IV. CONCLUSIONS

In this work, we have examined whether the oscillatory behavior of the gravitational potential of DM halos predicted by some DM scenarios could be detected by gravitational wave interferometers such as LISA and DECIGO, if binary systems were embedded within high-density DM clouds. Building on the early work in Ref. [47], which considered the impact of these oscillations on pulsar timing signals, we now consider their impact on the phase of the GW form received by interferometers. We derived the associated phase shift and performed a Fisher analysis to estimate the detection thresholds that can be expected for near future instruments, for a variety of binary systems.

We find that this probe is unlikely to be competitive with more direct observations of DM substructures. For $m_\phi > 10^{-21}$ eV the effect of the DM environment on the GW form due to the usual dynamical friction (the drag

force that contributes to the shrinking of the orbital radius of the binary system) is expected to dominate over the effect associated with these oscillatory features of the DM gravitational potential (which only affect a subleading component of Ψ_N). For low particle masses below 10^{-23} eV, the scalar clouds are associated with Compton wavelengths greater than the parsec scale. This implies DM clouds that are too large to provide realistic DM scenarios.

For DM masses $m_\phi \sim 10^{-22}$ eV, the phase shift associated with the oscillations of the DM gravitational potential can only be detected by LISA or DECIGO for densities that are greater than that in the solar neighborhood by a factor 10^5 (LISA) or 10^4 (DECIGO). This would also correspond to cloud masses above $10^5 M_\odot$ (LISA) or $10^3 M_\odot$ (DECIGO) and radii above 0.4 pc. Although such high-density structures may be possible, if they formed at redshifts $z \sim 10^4$, this would require a non-standard formation mechanism, such as instabilities due to DM self-interactions. In this sense, LISA and DECIGO would only be sensitive to the oscillatory features from exotic types of DM.

Therefore, except for a small region in the parameter space of DM models, the phase of the GW wave form is unlikely to be sensitive to the oscillatory features of DM gravitational potentials. This justifies standard analyses of the emission of GWs by binary systems, where the DM environment is neglected or considered through its usual effects: dynamical friction, accretion and gravitational pull by the enclosed DM mass within the orbital radius. On the other hand, from a beyond the standard model perspective, LISA and DECIGO could provide us with a window on the physics of dark matter and its possible exotic properties in the radiation era before large scale structures of the Universe form.

ACKNOWLEDGEMENTS

This work was partially supported by the MICINN (Ministerio de Ciencia e Innovación, Spain) projects PID2019-107394GB-I00/AEI/10.13039/501100011033 (AEI/FEDER, UE) and PID2022-139841NB-I00, COST (European Cooperation in Science and Technology) Actions CA21106 and CA21136. J.A.R.C. acknowledges support by Institut Pascal at Université Paris-Saclay during the Paris-Saclay Astroparticle Symposium 2022, with the support of the P2IO Laboratory of Excellence (program “Investissements d’avenir” ANR-11-IDEX-0003-01 Paris-Saclay and ANR-10-LABX-0038), the P2I axis of the Graduate School of Physics of Université Paris-Saclay, as well as IJCLab, CEA, APPEC, IAS, OSUPS, and the IN2P3 master project UCMN. C.B. is supported by the STFC under grant ST/T000732/1.

- [1] L. Hui, J. P. Ostriker, S. Tremaine, and E. Witten, *Phys. Rev. D* **95**, 043541 (2017), 1610.08297.
- [2] N. Bar, D. Blas, K. Blum, and S. Sibiryakov, *Phys. Rev. D* **98**, 083027 (2018), 1805.00122.
- [3] J. A. R. Cembranos, A. L. Maroto, and S. J. Núñez Jareño, *JHEP* **03**, 013 (2016), 1509.08819.
- [4] M. S. Turner, *Phys. Rev. D* **28**, 1243 (1983).
- [5] M. C. Johnson and M. Kamionkowski, *Phys. Rev. D* **78**, 063010 (2008), 0805.1748.
- [6] P. Brax, J. A. R. Cembranos, and P. Valageas, *Phys. Rev. D* **100**, 023526 (2019), 1906.00730.
- [7] W. Hu, R. Barkana, and A. Gruzinov, *Physical Review Letters* **85**, 1158 (2000), ISSN 00319007.
- [8] H. Y. Schive, T. Chiueh, and T. Broadhurst, *Nature Physics* **10**, 496 (2014), ISSN 17452481.
- [9] P. Mocz, M. Vogelsberger, V. H. Robles, J. Zavala, M. Boylan-Kolchin, A. Fialkov, and L. Hernquist, *Monthly Notices of the Royal Astronomical Society* **471**, 4559 (2017), ISSN 13652966.
- [10] S. May and V. Springel, *Monthly Notices of the Royal Astronomical Society* **506**, 2603 (2021), ISSN 0035-8711, URL <https://academic.oup.com/mnras/article/506/2/2603/6308377>.
- [11] A. V. Macciò, S. Paduroiu, D. Anderhalden, A. Schneider, and B. Moore, *Monthly Notices of the Royal Astronomical Society* **424**, 1105 (2012), ISSN 13652966, URL <https://academic.oup.com/mnras/article/424/2/1105/998349>.
- [12] D. H. Weinberg, J. S. Bullock, F. Governato, R. Kuzio de Naray, and A. H. G. Peter, *Proceedings of the National Academy of Science* **112**, 12249 (2015).
- [13] J. S. Bullock and M. Boylan-Kolchin, *Annual Review of Astronomy and Astrophysics* **55**, 343 (2017).
- [14] A. Del Popolo and M. Le Delliou, *Galaxies* **5**, 17 (2017).
- [15] P. Mocz, A. Fialkov, M. Vogelsberger, F. Becerra, M. A. Amin, S. Bose, M. Boylan-Kolchin, P. H. Chavanis, L. Hernquist, L. Lancaster, et al., *Physical Review Letters* **123**, 141301 (2019), ISSN 10797114, URL <https://journals.aps.org/prl/abstract/10.1103/PhysRevLett.123.141301>.
- [16] P. Mocz, A. Fialkov, M. Vogelsberger, F. Becerra, X. Shen, V. H. Robles, M. A. Amin, J. Zavala, M. Boylan-Kolchin, S. Bose, et al., *Monthly Notices of the Royal Astronomical Society* **494**, 2027 (2020), ISSN 0035-8711, URL <https://academic.oup.com/mnras/article/494/2/2027/5819969>.
- [17] S. Banerjee, S. Bera, and D. F. Mota, *Journal of Cosmology and Astroparticle Physics* **2020**, 034 (2020), ISSN 1475-7516, URL <https://iopscience.iop.org/article/10.1088/1475-7516/2020/07/034https://iopscience.iop.org/article/10.1088/1475-7516/2020/07/034/meta>.
- [18] M. Mina, D. F. Mota, and H. A. Winther, *Astronomy & Astrophysics* **662**, A29 (2022), ISSN 0004-6361, URL https://www.aanda.org/articles/aa/full_html/2022/06/aa38876-20/aa38876-20.htmlhttps://www.aanda.org/articles/aa/abs/2022/06/aa38876-20/aa38876-20.html.
- [19] X. Li, L. Hui, and T. D. Yavetz, *Physical Review D* **103** (2021), ISSN 24700029.
- [20] L. Hui, *Annual Review of Astronomy and Astrophysics* **59**, 247 (2021), ISSN 00664146, URL <https://www.annualreviews.org/doi/abs/10.1146/annurev-astro-120920-010024>.
- [21] T. P. Woo and T. Chiueh, *The Astrophysical Journal* **697**, 850 (2009), ISSN 0004-637X, URL <https://iopscience.iop.org/article/10.1088/0004-637X/697/1/850https://iopscience.iop.org/article/10.1088/0004-637X/697/1/850/meta>.
- [22] D. J. Marsh and J. C. Niemeyer, *Physical Review Letters* **123** (2019), ISSN 10797114.
- [23] J. Veltmaat, J. C. Niemeyer, and B. Schwabe, *Physical Review D* **98** (2018), ISSN 24700029.
- [24] N. Glennon and C. Prescod-Weinstein, *Physical Review D* **104**, 083532 (2021), ISSN 24700029, URL <https://journals.aps.org/prd/abstract/10.1103/PhysRevD.104.083532>.
- [25] P.-H. Chavanis, *Physical Review D* **84**, 043531 (2011), ISSN 15507998.
- [26] P.-H. Chavanis and L. Delfini, *Physical Review D* **84**, 043532 (2011), ISSN 1550-7998, URL <https://journals.aps.org/prd/abstract/10.1103/PhysRevD.84.043532>.
- [27] T. Rindler-Daller and P. R. Shapiro, *Monthly Notices of the Royal Astronomical Society* **422**, 135 (2012).
- [28] B. Li, T. Rindler-Daller, and P. R. Shapiro, *Physical Review D - Particles, Fields, Gravitation and Cosmology* **89**, 083536 (2014), ISSN 15502368, URL <https://journals.aps.org/prd/abstract/10.1103/PhysRevD.89.083536>.
- [29] B. Li, P. R. Shapiro, and T. Rindler-Daller, *Physical Review D* **96**, 063505 (2017), ISSN 24700029, URL <https://journals.aps.org/prd/abstract/10.1103/PhysRevD.96.063505>.
- [30] V. Desjacques, A. Kehagias, and A. Riotto, *Physical Review D* **97**, 023529 (2018).
- [31] P.-H. Chavanis, *Physical Review D* **103**, 123551 (2021).
- [32] S. T. Hartman, H. A. Winther, and D. F. Mota, *Journal of Cosmology and Astroparticle Physics* **2022**, 005 (2022), ISSN 1475-7516, URL <https://iopscience.iop.org/article/10.1088/1475-7516/2022/02/005https://iopscience.iop.org/article/10.1088/1475-7516/2022/02/005/meta>.
- [33] S. T. H. Hartman, H. A. Winther, and D. F. Mota, *Astronomy & Astrophysics* **666**, A95 (2022), ISSN 0004-6361, URL https://www.aanda.org/articles/aa/full_html/2022/10/aa43496-22/aa43496-22.htmlhttps://www.aanda.org/articles/aa/abs/2022/10/aa43496-22/aa43496-22.html.
- [34] P. Mocz, A. Fialkov, M. Vogelsberger, M. Boylan-Kolchin, P.-H. Chavanis, M. A. Amin, S. Bose, T. Dome, L. Hernquist, L. Lancaster, et al., *Monthly Notices of the Royal Astronomical Society* **521**, 2608 (2023), ISSN 0035-8711, URL <https://academic.oup.com/mnras/article/521/2/2608/7070733>.
- [35] S. Chakrabarti, B. Dave, K. Dutta, and G. Goswami, *Journal of Cosmology and Astroparticle Physics* **2022**, 074 (2022), URL <https://dx.doi.org/10.1088/1475-7516/2022/09/074>.
- [36] B. Dave and G. Goswami, *Journal of Cosmology and Astroparticle Physics* **2023**, 015 (2023), URL <https://>

- [dx.doi.org/10.1088/1475-7516/2023/07/015](https://doi.org/10.1088/1475-7516/2023/07/015).
- [37] P.-H. Chavanis, *Astron. Astrophys.* **537**, A127 (2012), 1103.2698.
- [38] P. Brax, J. A. R. Cembranos, and P. Valageas, *Phys. Rev. D* **102**, 083012 (2020), 2007.04638.
- [39] P. Amaro-Seoane et al. (LISA) (2017), 1702.00786.
- [40] S. Kawamura et al., *PTEP* **2021**, 05A105 (2021), 2006.13545.
- [41] R. Vicente and V. Cardoso, *Phys. Rev. D* **105**, 083008 (2022), 2201.08854.
- [42] V. Cardoso and A. Maselli, *Astron. Astrophys.* **644**, A147 (2020), 1909.05870.
- [43] J. Bamber, J. C. Aurrekoetxea, K. Clough, and P. G. Ferreira (2022), 2210.09254, URL <https://arxiv.org/pdf/2210.09254.pdf>.
- [44] D. Traykova, R. Vicente, K. Clough, T. Helfer, E. Berti, P. G. Ferreira, and L. Hui (2023), 2305.10492, URL <https://arxiv.org/pdf/2305.10492.pdf>.
- [45] A. Boudon, P. Brax, P. Valageas, and L. K. Wong (2023), 2305.18540.
- [46] J. C. Aurrekoetxea, K. Clough, J. Bamber, and P. G. Ferreira (2023), 2311.18156, URL <https://arxiv.org/pdf/2311.18156.pdf>.
- [47] A. Khmelnitsky and V. Rubakov, *JCAP* **02**, 019 (2014), 1309.5888.
- [48] S. Chandrasekhar, *Astrophys. J.* **97**, 255 (1943).
- [49] E. Barausse, V. Cardoso, and P. Pani, *Phys. Rev. D* **89**, 104059 (2014), 1404.7149.
- [50] A. Lamberts, S. Blunt, T. B. Littenberg, S. Garrison-Kimmel, T. Kupfer, and R. E. Sanderson, *Mon. Not. Roy. Astron. Soc.* **490**, 5888 (2019), 1907.00014.
- [51] N. Seto, *Phys. Rev. Lett.* **128**, 041101 (2022), 2201.03685.
- [52] E. Poisson and C. M. Will, *Gravity: Newtonian, Post-Newtonian, Relativistic* (Cambridge University Press, 2014).
- [53] E. Poisson and C. M. Will, *Phys. Rev. D* **52**, 848 (1995), gr-qc/9502040.
- [54] M. Vallisneri, *Phys. Rev. D* **77**, 042001 (2008), gr-qc/0703086.
- [55] B. P. Abbott et al. (LIGO Scientific, Virgo), *Phys. Rev. X* **9**, 031040 (2019), 1811.12907.